SUPPLEMENTARY MATERIAL
Influence of compatible solute ectoine on distinct DNA structures: thermodynamic insights into molecular binding mechanisms and destabilization effects

Ewa Anna Oprzeska-Zingrebe,* Susann Meyer,† Alexander Roloff,‡ Hans-Jörg Kunte§ and Jens Smiatek¶

2018

1 Snapshots of the initial conformations of 7-bp DNA oligonucleotide (PDB ID: 1KR8)

1.1 1KR8 DNA hairpin in the native form

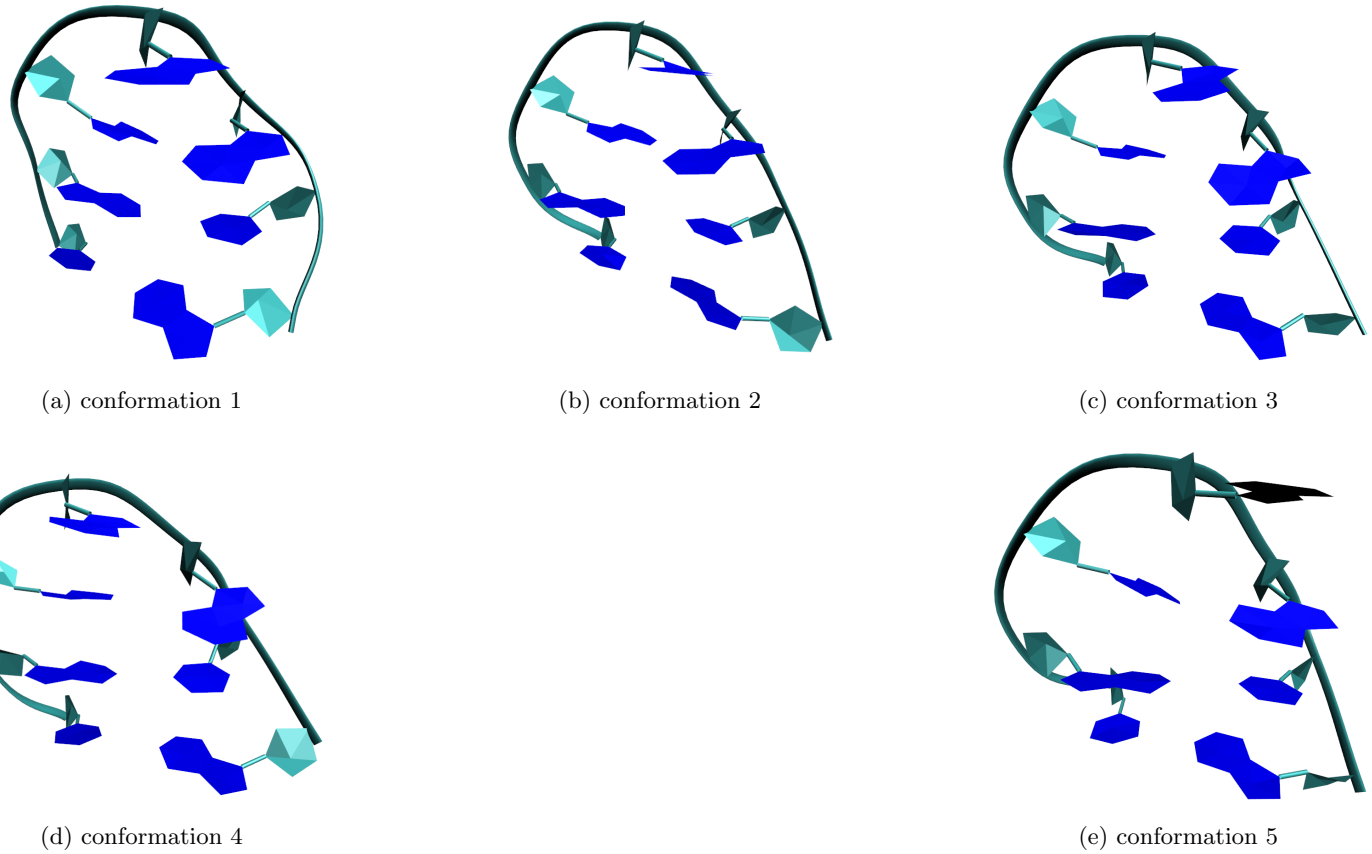

(a) conformation 1 (b) conformation 2 (c) conformation 3

(d) conformation 4 (e) conformation 5

Figure 1: Snapshots of the initial conformations of 1KR8 DNA hairpin in its native form.

*Institute for Computational Physics, University of Stuttgart, Allmandring 3, D-70569 Stuttgart, Germany.
†Federal Institute for Materials Research and Testing, Unter den Eichen 87, D-12205 Berlin, Germany.
‡Federal Institute for Materials Research and Testing, Unter den Eichen 87, D-12205 Berlin, Germany.
§Federal Institute for Materials Research and Testing, Unter den Eichen 87, D-12205 Berlin, Germany.
¶Helmholtz Institute Münster: Ionics in Energy Storage (HI MS IEK-12), Forschungszentrum Jülich GmbH, Corrensstrasse 46, D-48149 Münster, Germany. Email: smiatek@icp.uni-stuttgart.de

1.2 1KR8 DNA hairpin in the unfolded form

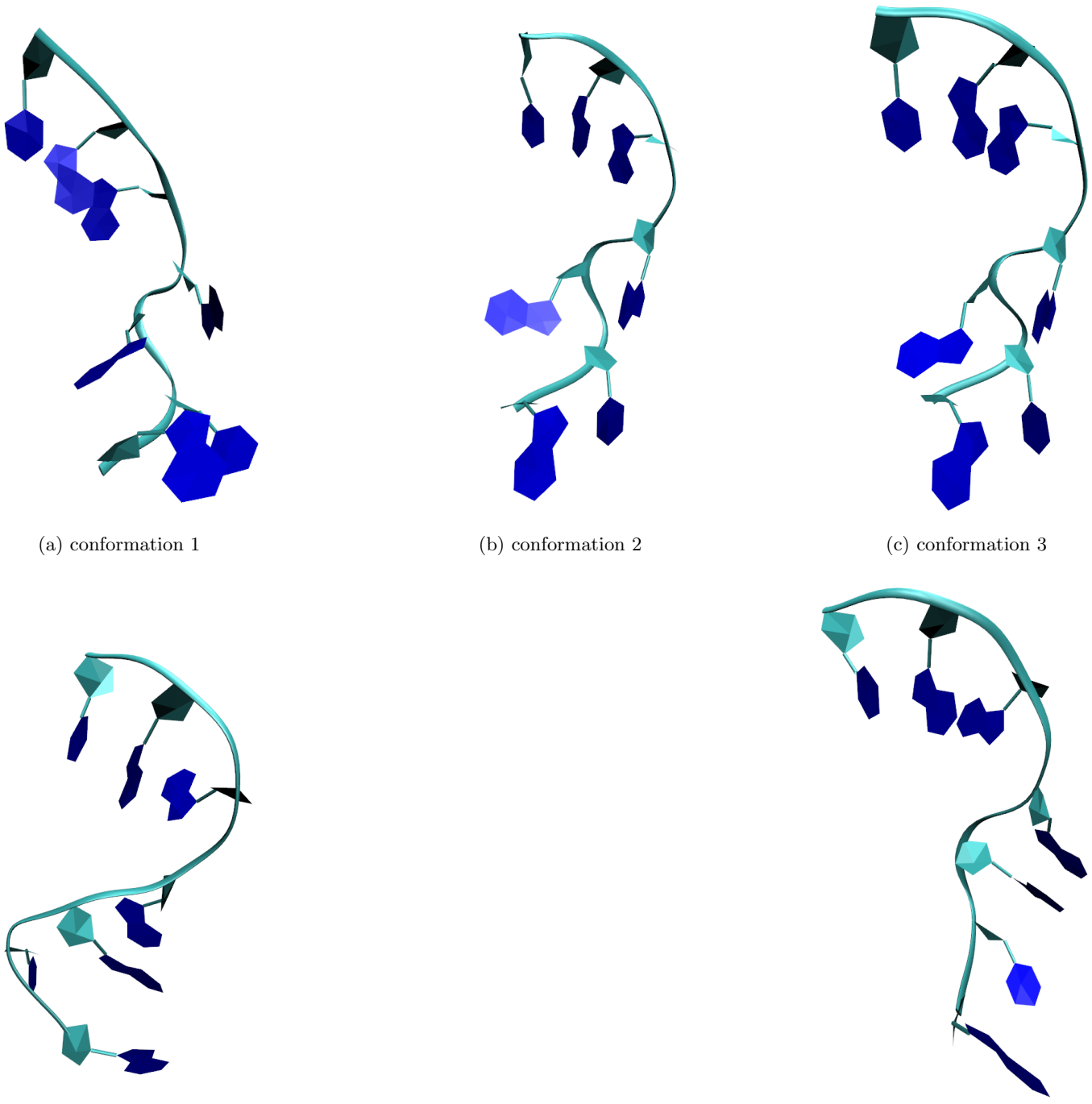

(a) conformation 1

(b) conformation 2

(c) conformation 3

(d) conformation 4

(e) conformation 5

Figure 2: Snapshots of the initial conformations of 1KR8 DNA hairpin in its unfolded form.

2 Details of the simulated systems

Number of ectoine molecules		ectoine concentration [mol/L]					
DNA form		0	0.5	1	1.5	2	3
native 1KR8	conformation 1	0	310	620	930	1240	1860
	conformation 2	0	330	660	990	1320	1980
	conformation 3	0	330	659	989	1319	1978
	conformation 4	0	331	662	993	1324	1987
	conformation 5	0	317	635	953	1270	1905
unfolded 1KR8	conformation 1	0	369	738	1106	1475	2213
	conformation 2	0	381	762	1143	1524	2286
	conformation 3	0	367	733	1100	1467	2200
	conformation 4	0	380	760	1139	1519	2279
	conformation 5	0	386	773	1160	1546	2319
B-DNA	conformation 1	0	589	1177	1766	2354	3531

Table 1: Number of ectoine molecules in the simulated systems for 1KR8 native and unfolded DNA and B-DNA in water.

Number of water molecules		ectoine concentration [mol/L]					
DNA form		0	0.5	1	1.5	2	3
native 1KR8	conformation 1	34195	31636	29116	26661	24201	19548
	conformation 2	36366	33653	30962	28335	25760	20809
	conformation 3	36337	33630	30951	28319	25739	20808
	conformation 4	36381	33674	30958	28348	25755	20798
	conformation 5	35161	32534	29964	27438	24961	20149
unfolded 1KR8	conformation 1	40739	37723	34699	31743	28869	23257
	conformation 2	42120	38987	35886	32858	29870	24141
	conformation 3	40441	37455	34456	31536	28686	23135
	conformation 4	41918	38774	35695	32682	29728	24005
	conformation 5	42593	39450	36303	33201	30200	24433
B-DNA	conformation 1	64545	59723	54971	50324	45738	36980

Table 2: Number of water molecules in the simulated systems for 1KR8 native and unfolded DNA and B-DNA for different ectoine concentrations.

Length of the simulation box [nm]		ectoine concentration [mol/L]					
DNA form		0	0.5	1	1.5	2	3
native 1KR8	conformation 1	10.14169	10.05548	9.96594	9.88794	9.81922	9.69530
	conformation 2	10.35056	10.25588	10.17374	10.09452	10.02147	9.89912
	conformation 3	10.34852	10.26622	10.17251	10.09007	10.02645	9.89968
	conformation 4	10.34998	10.25867	10.17743	10.10575	10.02404	9.90219
	conformation 5	10.23340	10.13819	10.06775	9.98973	9.90859	9.78998
unfolded 1KR8	conformation 1	10.74297	10.65081	10.57435	10.48175	10.40657	10.26652
	conformation 2	10.86500	10.77365	10.68824	10.60640	10.53664	10.39221
	conformation 3	10.72111	10.62127	10.53937	10.46173	10.39184	10.25752
	conformation 4	10.84940	10.76418	10.66875	10.59256	10.51176	10.38027
	conformation 5	10.90201	10.80914	10.73230	10.64403	10.56890	10.44390
B-DNA	conformation 1	12.53180	12.42371	12.33240	12.23447	12.14858	12.00295

Table 3: Length of the simulation box edge in [nm] for all the systems studied.

3 Convergence of Kirkwood-Buff integrals

In order to demonstrate the validity of the Kirkwood-Buff integrals, we evaluated the time behavior for the ectoine-ectoine and ectoine-water integrals regarding the 0.5 mol/L ectoine-water solution in absence of DNA.

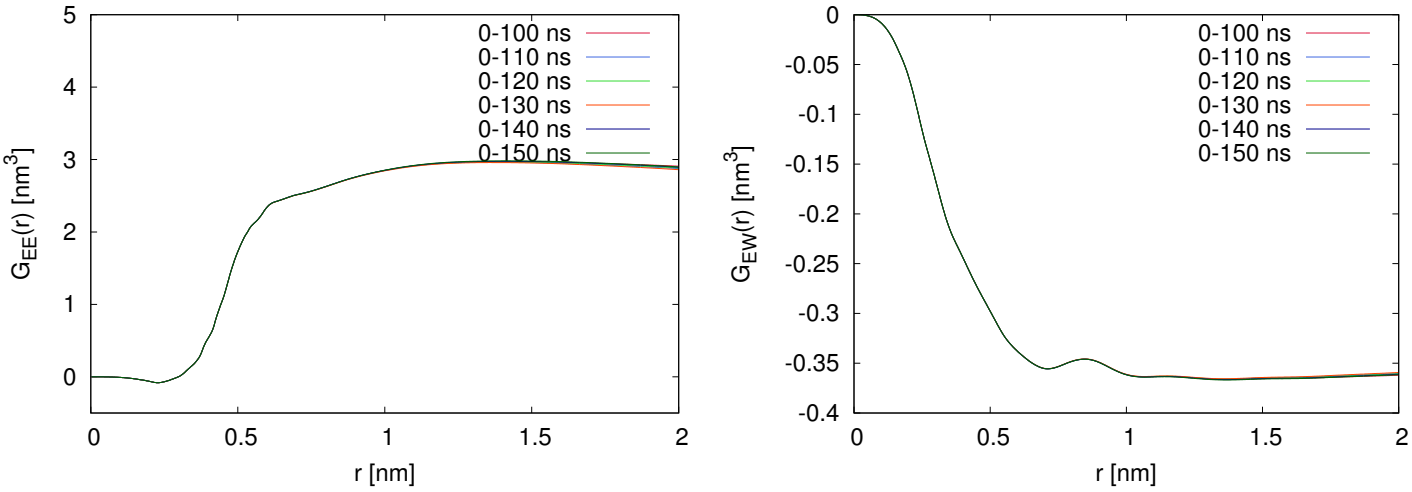

Figure 3: Running Kirkwood-Buff integrals for different concentrations of ectoine as denoted in the legend around DNA 1KR8 native (left side) and unfolded conformations (right side). The solid lines represent the respective mean values of 5 independent restraint simulation runs with slightly different DNA conformations.

4 Solvation number around ectoine

The solvation number of water molecules around ectoine can be calculated in accordance with the coordination number (Eqn. (3)) in the main text. As a matter of definition, the solvation number is defined at well defined distances r_1, and r_2, which can be associated with corresponding solvation shells. The solvation shells can be determined from the center-of-mass radial distribution functions between ectoine and water molecules, which are shown in Fig. 4.

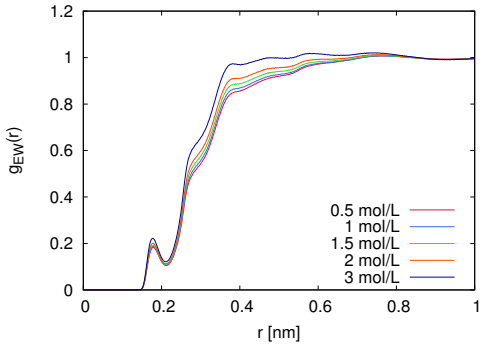

Figure 4: Center-of-mass radial distribution function of water molecules around ectoine at different ectoine concentrations.

In order to define the number of strongly Z_b and weakly bound water molecules Z_{ib} in accordance with Ref. [1], we determine the corresponding solvation shells from Fig. 4 at $r_1 = 0.308$ nm for Z_b, and $r_2 = 0.408$ nm for Z_{ib} as most evident peaks from the radial distribution functions. The running solvation numbers are shown in Fig. 5.

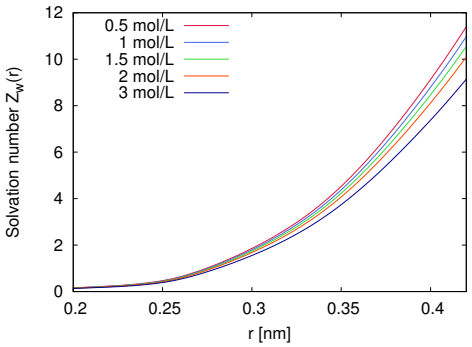

Figure 5: Running solvation numbers between ectoine and water molecules for different ectoine concentrations.

The corresponding discrete values for Z_b, an for Z_{ib} at r_1 and r_2 in comparison to experimental data [1] are shown in Fig. 6. The values are in qualitiative agreement with the experimental data. It has to be noted that the maximum error in the experiments is $\Delta Z_i = \pm 2$, which highlights the validity of our force field in terms of hydration behavior [1].

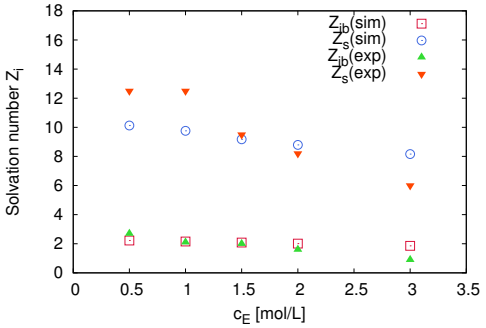

Figure 6: Solvation numbr for strongly bound and weakly bound solvation numbers in comparison to experimental data. The values for the experimental data have a maximum error of $\Delta Z_i = \pm 2$.

5 Preferential binding coefficients between ectoine and DNA

The distance-dependent preferential binding coefficients between DNA and ectoine are calculated according to the relation

$$\nu_{23}(r) = \rho_3(G_{23}(r) - G_{21}(r)) \tag{1}$$

and the corresponding results for unfolded and native 1KR8 DNA conformations are shown in Fig. 7.

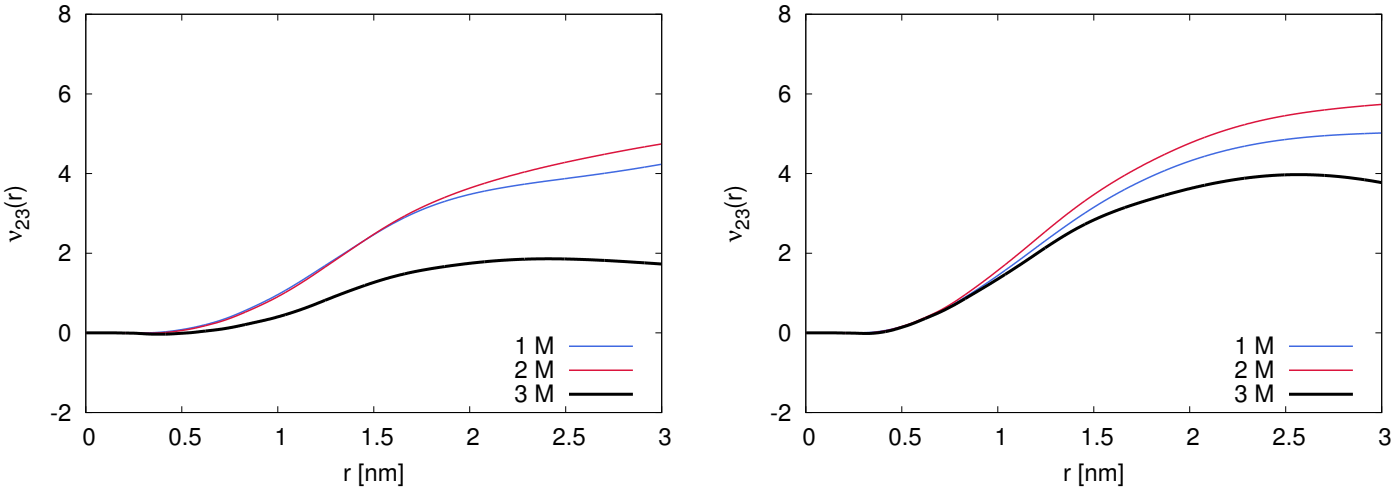

Figure 7: Running preferenital binding coefficients for for different concentrations of ectoine as denoted in the legend around DNA 1KR8 native (left side) and unfolded conformations (right side).

The corresponding results for B-DNA and ectoine are shown in Fig. 8. Here, only one simulation was performed for each concentration.

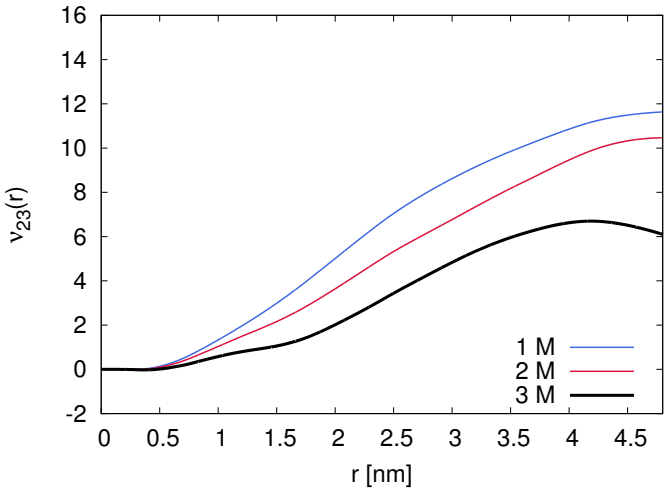

Figure 8: Running preferential binding coefficients $\nu_{23}(r)$ for ectoine around B-DNA for different ectoine concentrations as denoted in the legend.

6 Kirkwood-Buff integrals between DNA and ectoine

The Kirkwood-Buff integrals $G_{23}(r)$ between folded/unfolded DNA hairpins and ectoine are shown in Fig. 9. The change from positive to negative values for the Kirkwood-Buff integrals highlights the saturation of the ectoine shell around DNA for ectoine concentrations $c_E \geq 2$ M.

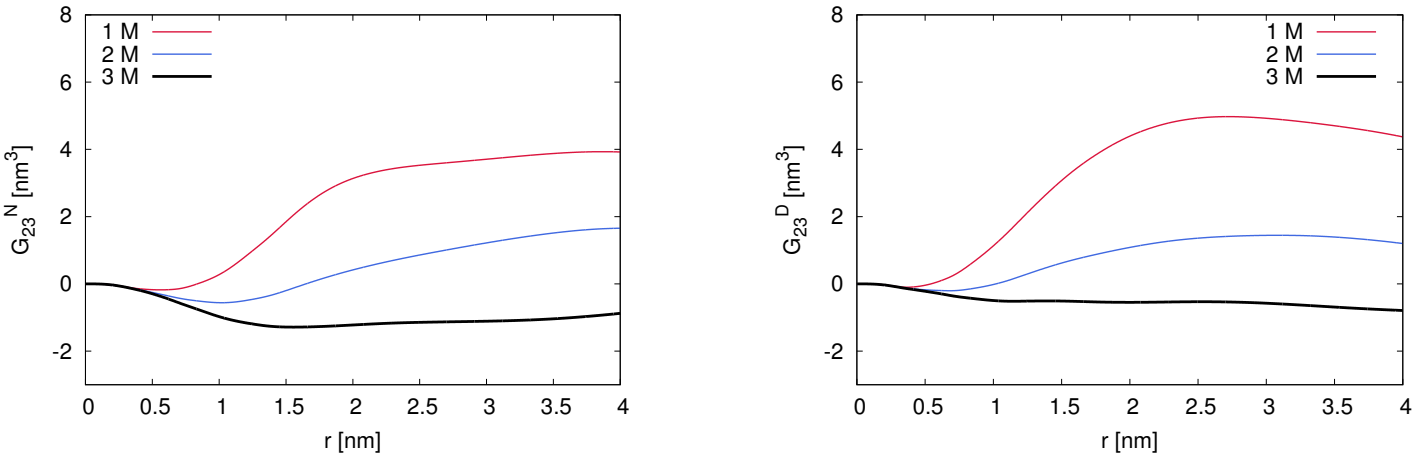

Figure 9: Running Kirkwood-Buff integrals between native (left side) and unfolded (right side) DNA hairpins and different concentrations of ectoine.

7 Derivative of the chemical activity for ectoine in water

In order to get an insight into the non-ideal effects of the simulated solution we calculated the derivative of chemical activity a_{EE} for ectoine in water, defined by the Eq. 2

$$a_{\mathrm{EE}} = \frac{1}{1 + \rho_{\mathrm{E}}(G_{\mathrm{EE}} - G_{\mathrm{EW}})} \tag{2}$$

where G_{EE} and G_{EW} stand for the ectoine-ectoine and the ectoine-water Kirkwood-Buff integrals. Hence, the ideal mixture is described by $a_{EE} = 1$, whereas the condition $a_{EE} \neq 1$ indicates the deviation from ideal behavior as discussed in more details in Ref. [2]. For this purpose we performed atomistic MD simulations of 150 ns length for 0.5-3 M ectoine in pure water with the same simulation protocol and setup as described in the main article for 1KR8 DNA hairpins. Contrary to DNA-ectoine simulations, we replaced DNA with water molecules to fill the free volume. The details of the simulated systems are given in Tab. 4.

ectoine concentration [mol/L]	**Number of ectoine molecules**	**Number of water molecules**	**Length of the simulation box [nm]**
0.5	301	30739	9.94642
1	602	28307	9.86667
1.5	903	25889	9.78912
2	1204	23518	9.72309
3	1807	18996	9.59940

Table 4: Details of the binary systems of ectoine in pure water for 0.5 - 3 M ectoine concentrations.

The resulting values for a_{EE} are presented in Fig. 10.

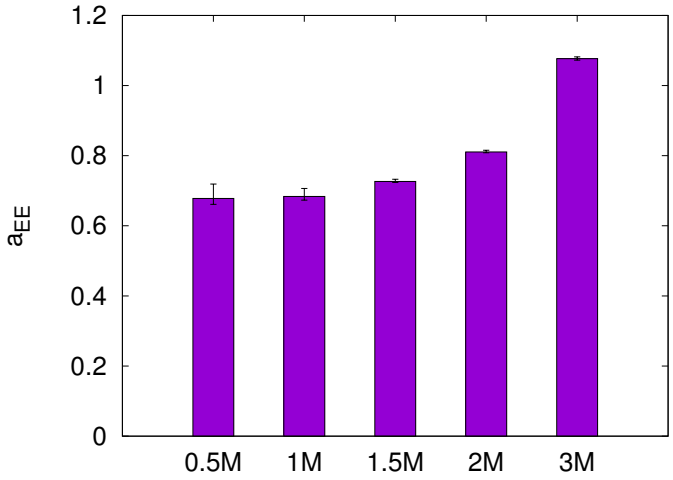

Figure 10: Derivative of the chemical activity a_{EE}.

The calculated a_{EE} values follow the pattern $a_{EE} \neq 1$, which reveals the slightly non-ideal behavior of the simulated mixture. The non-ideality of distribution is more pronounced for lower ectoine concentrations. With reference to Eq. 2 it can be observed, that $G_{EW} > G_{EE}$ due to $a_{EE} < 1$. It can be thus concluded, that the hydration properties of zwitterionic ectoine molecules in our systems are well pronounced, as well as that the cluster formation tendency of ectoine molecules is relatively weak.

8 Ratio of ectoine-DNA hydrogen bonds to the total number of hydrogen bonds

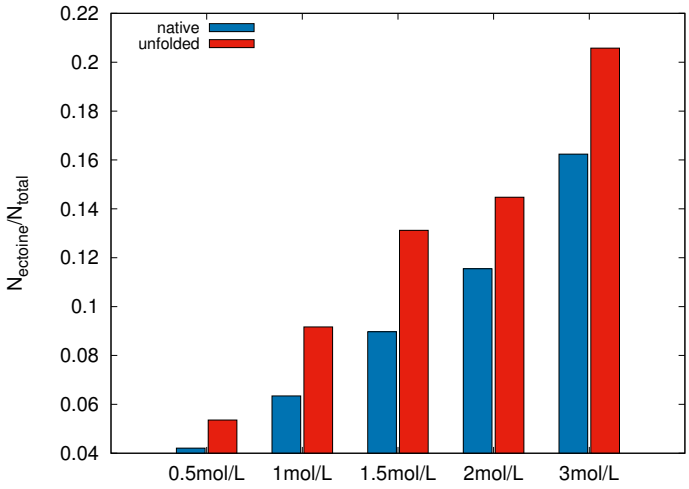

Figure 11: Number of DNA-ectoine hydrogen bonds for native and unfolded 1KR8 DNA form $N_{ectoine}$ divided by the total number of hydrogen bonds N_{total} for different ectoine concentrations.

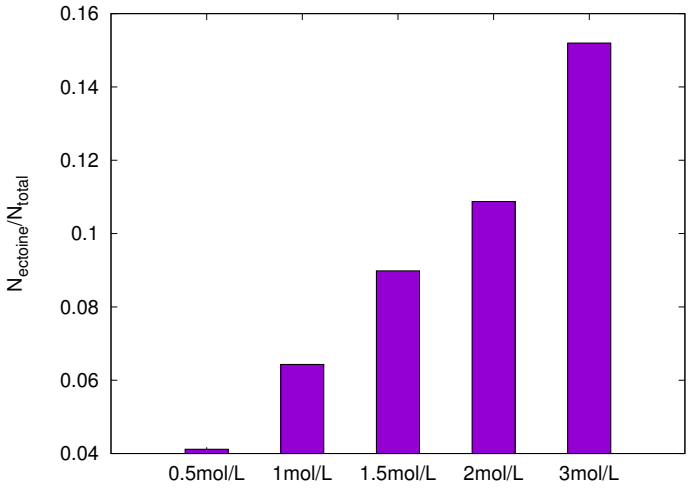

Figure 12: Number of DNA-ectoine hydrogen bonds for B-DNA $N_{ectoine}$ divided by the total number of hydrogen bonds N_{total} for different ectoine concentrations.

9 Solvent orientation parameters

To investigate the possible influence of ectoine on the local hydration shell, one can study the angular distribution of water molecules around DNA, expressed via solvent orientation parameters f_1 and f_2 [3]. The corresponding equations read

$$f_1 = \langle \cos\, \theta_1 \rangle \tag{3}$$

and

$$f_2 = \langle 3\cos^2\, \theta_2 - 1 \rangle \tag{4}$$

where the angle θ_1 is spanned between the vector from a water hydrogen atom to the midpoint between the oxygen and a further hydrogen atom of a different water molecule, and the angle θ_2 is extended between the surface of the solute and the normal of the water molecule plane. Both solvent orientation parameters provide a rational insight into the local arrangement of water molecules around DNA in the presence of ectoine.

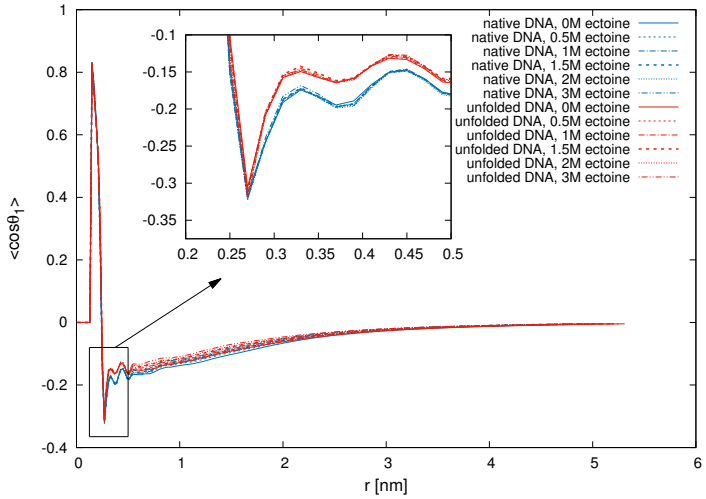

Figure 13: Water order parameter f_1 according to Eq. 3 for water molecules around 1KR8 7-bp DNA oligonucleotide in its native and unfolded form for varying ectoine concentrations. The inset represents the close-up of the selected part of the graph as pointed by the arrow.

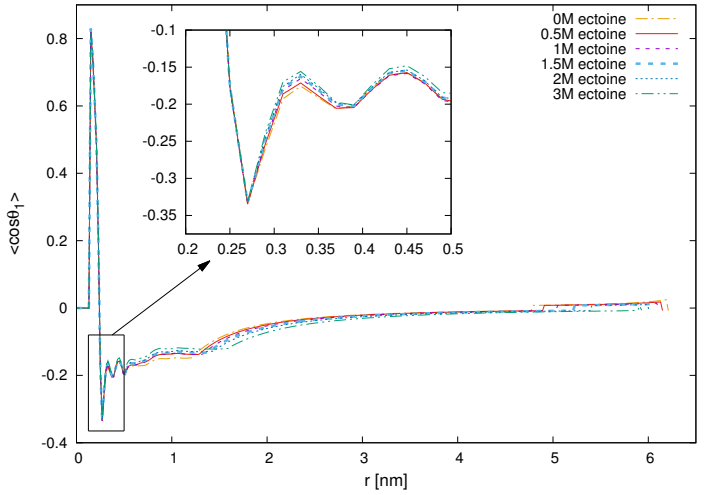

Figure 14: Water order parameter f_1 according to Eq. 3 for water molecules around B-DNA structure for varying ectoine concentrations. The inset represents the close-up of the selected part of the graph as pointed by the arrow.

Our results show, that the orientation of water molecules at short distances around DNA remains almost unaffected in the presence of ectoine as compared to the pure water and DNA solution. Slight deviations can be observed only at the distances of 0.5-3 nm for B-DNA (Fig.14) and 0.5-2.5 nm for 1KR8 oligonucleotides (Fig. 13), which corresponds to the higher order

solvation shells. Since ectoine, which is preferentially bound within the first solvation shell around DNA, appears to exert only marginal influence on the orientation of water molecules, the indirect mechanism of DNA-ectoine interaction involving the pronounced changes in water structure can be with good approximation disregarded.

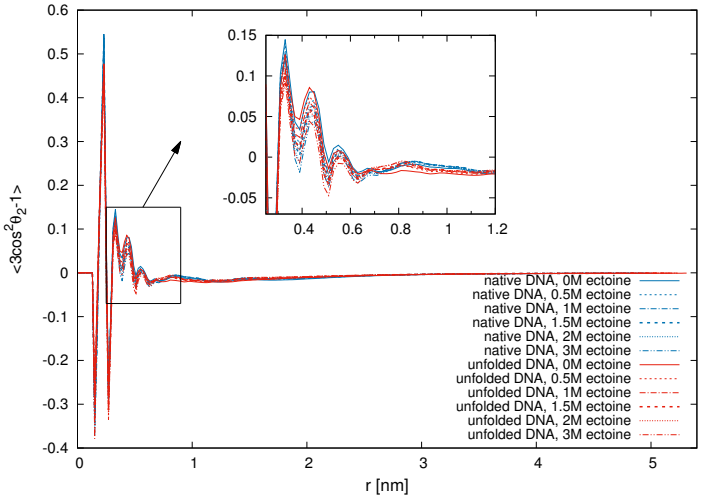

Figure 15: Water order parameter f_2 according to Eq. 4 for water molecules around 1KR8 7-bp DNA oligonucleotide in its native and unfolded form for varying ectoine concentrations. The inset represents the close-up of the selected part of the graph as pointed by the arrow.

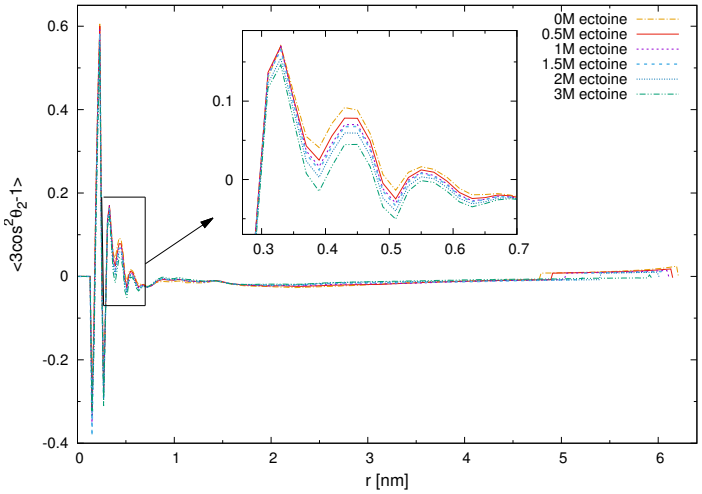

Figure 16: Water order parameter f_2 according to Eq. 4 for water molecules around B-DNA structure for varying ectoine concentrations. The inset represents the close-up of the selected part of the graph as pointed by the arrow.

Additional support to the direct mechanism of DNA-ectoine interaction comes from the analysis of water order parameter f_2. Similarly to f_1, also here the influence of ectoine on local water structure is negligible regardless of ectoine concentration and involves only the distances $r > 4.5$ nm corresponding to the second- and higher order hydration shells. Taking into consideration all our findings it can be concluded, that DNA-ectoine binding occurs via direct mechanism involving the formation of hydrogen bonds and not by indirectly altering water structure in the vicinity of biomolecular surface.

10 Change of DNA melting temperatures

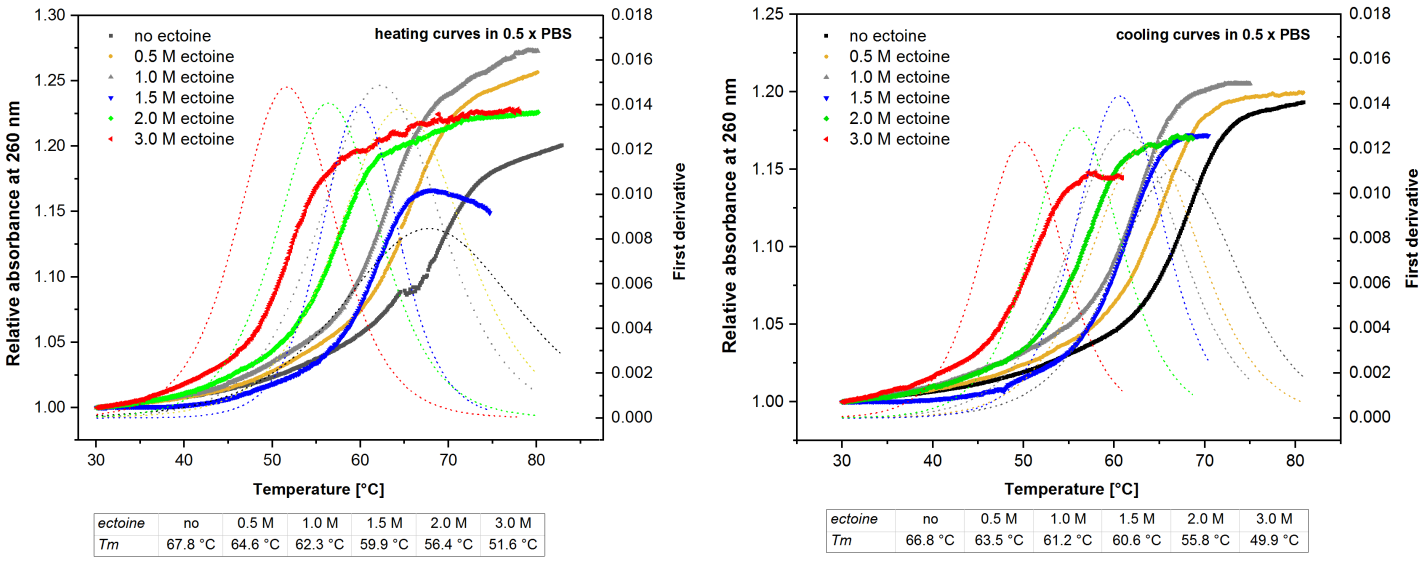

ectoine	no	0.5 M	1.0 M	1.5 M	2.0 M	3.0 M
Tm	67.8 °C	64.6 °C	62.3 °C	59.9 °C	56.4 °C	51.6 °C

ectoine	no	0.5 M	1.0 M	1.5 M	2.0 M	3.0 M
Tm	66.8 °C	63.5 °C	61.2 °C	60.6 °C	55.8 °C	49.9 °C

Figure 17: Representative plots of dsDNA (20 base pairs, GC = 65%) in each ectoine concentration showing the relative absorbance at 260 nm and the corresponding first derivative as function of temperature. The melting temperatures were determined via first derivative of Boltzmann fits and can be noted as similar and comparable concerning the melting curves during cooling and heating.

References

[1] A. Eiberweiser, A. Nazet, S. E. Kruchinin, M. V. Fedotova, and R. Buchner, "Hydration and ion binding of the osmolyte ectoine," *J. Phys. Chem. B*, vol. 119, no. 49, pp. 15203–15211, 2015.

[2] A. N. Krishnamoorthy, J. Zeman, C. Holm, and J. Smiatek, "Preferential solvation and ion association properties in aqueous dimethyl sulfoxide solutions," *Phys. Chem. Chem. Phys.*, vol. 18, no. 45, pp. 31312–31322, 2016.

[3] D. K. Hore, D. S. Walker, and G. L. Richmond, "Water at hydrophobic surfaces: when weaker is better," *J. Am. Chem. Soc.*, vol. 130, no. 6, pp. 1800–1801, 2008.